Alcian blue staining to track the intracellular fate of hyaluronic-acid-based nanoparticles at transmission electron microscopy

Flavia Carton,[1] Mathieu Repellin,[1] Giovanna Lollo,[2] Manuela Malatesta[1]

[1]Department of Neurosciences, Biomedicine and Movement Sciences, Anatomy and Histology Section, University of Verona, Italy
[2]Laboratory of Automatic Control, Chemical and Pharmaceutical Engineering (LAGEPP), French National Centre for Scientific Research (CNRS), UMR 5007, Claude Bernard University Lyon 1, Villeurbanne, France

Abstract

The main step in the assessment of nanomaterial safety and suitability for biomedical use is the location and the dynamic tracking of nanoparticles (NPs) inside cells or tissues. To precisely investigate the uptake mechanisms and intracellular fate of NPs, transmission electron microscopy is the technique of choice; however, the detection of NPs may sometimes be problematic. In fact, while NPs containing strongly electron dense (*e.g.* metal) components do not require specific detection methods at the ultrastructural level, organic NPs are hardly detectable in the intracellular environment due to their intrinsic moderate electron density. In this study, the critical-electrolyte-concentration Alcian Blue method set up by Schofield *et al.* in 1975 was applied to track hyaluronic-acid-based NPs in muscle cells *in vitro*. This long-established histochemical method proved to be a powerful tool allowing to identify not only whole NPs while entering cells and moving into the cytoplasm, but also their remnants following lysosomal degradation and extrusion.

Introduction

During the last two decades, a massive number of nanoparticles (NPs) have been developed with an increasing interest towards biomedical applications. Innovative nanoparticulate systems have been investigated as *e.g.* drug carriers, hyperthermia-inducing tools, contrast agents, biosensors, sorting systems, scaffold components.[1-13] As an obvious consequence, extensive *in vitro* and *in vivo* tests have been applied to assess the suitability of the nanosystems for their use in the biological media and their functional efficacy. To assess their toxicological profile, NPs are commonly visualised and tracked inside cells or tissues by conventional or confocal fluorescence microscopy using fluorescent markers.[14] To precisely investigate the uptake mechanisms and intracellular fate of NPs, transmission electron microscopy (TEM) is the technique of choice, although the detection of NPs may sometimes be problematic. NPs containing strongly electron dense components (*e.g.*, iron, silver, gold, silica) do not require specific detection methods,[15-18] while fluorescently-labelled nanoconstructs with intrinsic moderate electron density (*e.g.*, lipid- or polymer-based NPs) can be made easily recognizable by applying techniques of diaminobenzidine (DAB) photo-oxidation.[19-20] However, this latter technique is not applicable to all fluorophores since the success of the reaction depends on the capability of the fluorescent agent to generate reactive oxygen species in their excited state; moreover, its application is unfruitful in the presence of fluorescent background or autofluorescent sample components.

Thanks to its high water-binding capacity, biocompatibility and degradability, and non-immunogenicity, hyaluronic acid (HA) is of a great interest in the development of nanoconstructs for a wide variety of biomedical applications, from molecular imaging to targeted drug delivery.[21-23]

In the frame of a study aimed at developing novel biocompatible HA-nanocarriers,[11] we observed that these HA-based NPs exhibit a homogeneous and weak electron-density that makes them hardly detectable in the intracellular milieu; unfortunately, the cell types used in our experiments (C2C12 immortalized murine muscle cells) showed a strong intrinsic autofluorescence that prevented to apply DAB photo-oxidation to locate fluorescently-labelled HA-NPs at TEM. We then decided to find an alternative detection method to track the internalization and intracellular traffic of these NPs at the ultrastructural level.

So far, the critical-electrolyte-concentration technique applied to the Alcian Blue (AB) staining is a long-established histochemical method to reveal glycosaminoglycans in tissue slices.[24] In 1975, Schofield and coll.[25] used this histochemically specific technique to localize and discriminate cartilage mucopolysaccharides at TEM; they also improved the Scott and Dorling's technique demonstrating that the use of low concentrations of AB after fixation resulted in a similar staining pattern as after the original technique (that required the sample fixation and staining be simultaneously performed). In addition, this post-fixation procedure enhanced dye staining by allowing its penetration in the whole sample thickness, whereas in the simultaneous fixation-staining method the reaction was confined to the sample periphery. The staining consisted in electron dense fine granules that did not mask the cellular structural components.

Based on the data present in the literature, we investigated an innovative application of the AB method staining: we originally applied the critical-electrolyte-concentration AB method set up by Schofield *et al.*[25] to unequivocally detect HA-based NPs administered to cultured cells which has been never tested before.

Materials and Methods

HA-NPs were prepared by polyelectrolyte complexation, mixing HA (Lifecore

Correspondence: Manuela Malatesta, Department of Neurosciences, Biomedicine and Movement Sciences, Anatomy and Histology Section, University of Verona, Strada Le Grazie 8, 37134 Verona, Italy.
Tel. +30.045.8027569.
E-mail: manuela.malatesta@univr.it

Acknowledgements: MR is a PhD student in receipt of a fellowship from the INVITE project of the University of Verona, (PhD Programme in Nanoscience and Advanced Technologies). This project has received funding from the European Union's Horizon 2020 Research and Innovation Programme under the Marie Skłodowska-Curie grant agreement No. 754345.

Contributions: FC and MR contributed equally to this work. All authors contributed to the study conception and design. FC and MR, performed experiments and analysed data; GL, supervised the project and analysed data; MM supervised the project, analysed data and wrote the first draft of the manuscript. All authors read and commented the manuscript, and approved its final version.

Key words: Nanocarriers; hyaluronate; histochemistry; ultrastructure.

Received for publication: 16 November 2019.
Accepted for publication: 11 December 2019.

European Journal of Histochemistry 2019; 63:3086
doi:10.4081/ejh.2019.3086

Biomedical, Chaska, MN, USA) and poly-arginine (PArg) (Polypeptide therapeutic solutions, Valencia, Spain) with a molar ratio HA/PArg of 5.77.[11] To obtain fluorescent HA-NPs, 10% of the HA was conjugated with fluoresceinamine (Sigma-Aldrich, Saint Louis, MA, USA) as previously described.[26] Dynamic light scattering was used to characterized HA-NPs in terms of hydrodynamic diameter, polydispersity index (PDI) and Zeta potential (ζ), using Zetasizer Nano ZS (Malvern Instruments Limited, Malvern, UK).

C2C12 myoblasts (an immortalized murine cell line purchased from ATCC® CRL-1772) were cultured in 75 cm² plastic flasks using Dulbecco's modified Eagle medium, supplemented with 10% (v/v) FBS, 1% (w/v) Glutamine, 0.5% (v/v) Amphotericin B, 100 units/mL of Penicillin-Streptomycin (Gibco, Waltham, MA, USA) and incubated at 37°C with 5% CO_2. Cells were trypsinized in 0.05% EDTA in PBS and seeded onto glass coverslips (12 mm in diameter) in 24-multiwell ($6x10^3$ cells per well). Twenty-four hours after seeding, the cells were treated with 107 µg/mL of either HA-NPs or fluorescent NPs for TEM and bright field/fluorescence microscopy, respectively. During the treatment the percentage of FBS was reduced to 5% (v/v) in order to avoid NPs aggregation. Briefly, cells were administered the HA-NPs for 2 h, then the medium was removed and some samples were immediately fixed (see below) while others were given fresh medium without NPs for further 22 h before being fixed. These experimental conditions were selected based on previous experiments on cultured muscle cells[27], since by this procedure the NPs that had not been uptaken by cells were removed from the medium, and it was possible to follow the intracellular fate of the HA-NPs internalised during the 2-h-incubation only. This avoids possible cell overloading for long post-incubation times, and limits the interference of a medium possibly modified by the presence of non-internalised NPs and/or the low FBS concentration (it is worth recalling that C2C12 myoblasts may differentiate into myotubes when FBS concentration is maintained low for long times[28]). Untreated cell samples were used as control.

For bright field and fluorescence microscopy, control cells and cells treated with fluorescent HA-NPs were fixed with 4% (v/v) paraformaldehyde in PBS, pH 7.4 for 30 min at room temperature. Cells were stained with 1% (w/v) Alcian blue 8GX (Sigma, Saint Louis, MO, USA) in 3 % (v/v) acetic acid for 2 h at room temperature, and differentiated in tap water;[25] the cells were counterstained with Nuclear fast red (Bio-Optica, Milan, Italy) for 5 min at room temperature, dehydrated through an ascending series of ethanol, cleared in xylene and finally mounted in Entellan (Merck Millipore). The samples were observed with an Olympus BX51 (Olympus Italia Srl, Milan, Italy) microscope using a 60x objective either under bright field conditions or in fluorescence (100 W mercury lamp) using a 450-480 nm exitation filter, 500 nm dichroic mirror, and 515 nm barrier filter. Images were recorded with an QICAM Fast 1394 digital camera (QImaging, Surrey, BC, Canada) and processed using Image-Pro Plus 7.0 software (Media Cybernetics Inc., Rockville, MD, USA).

Fluorescent HA-NPs were also stained in suspension: briefly, 100 µL of AB solution were mixed with an equal volume of NPs solution for 2 h at room temperature. A drop of suspension of these AB-stained HA-NPs was placed onto a glass slide under a coverslip, and observed at the microscope, under the same conditions as above.

For TEM, control cells and cells treated with HA-NPs were fixed with 3% (v/v) glu-

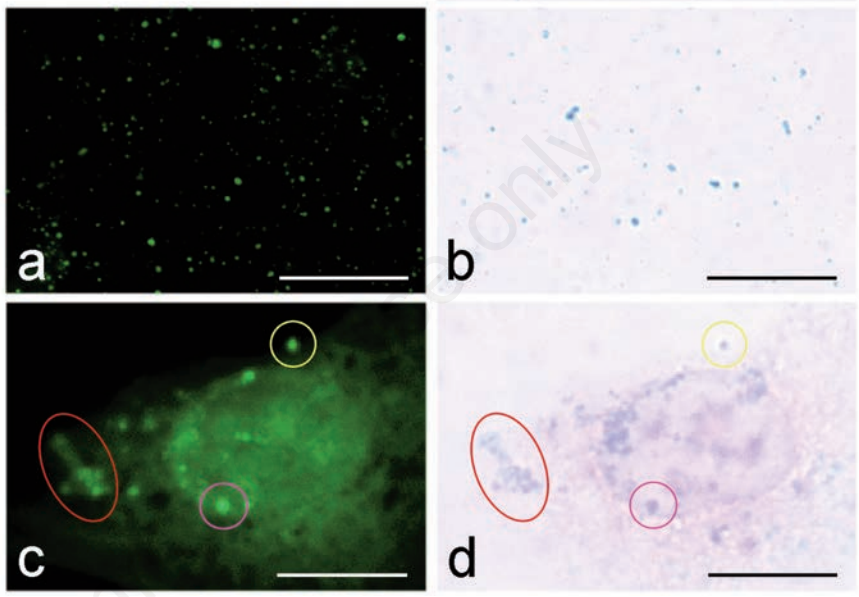

Figure 1. Fluoresceinamine-labelled HA-NPs in suspension as observed at conventional fluorescence microscopy (a) and bright field microscopy after staining with AB (b). c,d) A C2C12 myoblast after 24 h incubation with fluoresceinamine-labelled HA-NPs: the fluorescent signal of NPs (c) mostly overlaps AB staining (d) (encircled areas). Note the high intracellular fluorescence background in (c). Scale bars: 10 µm.

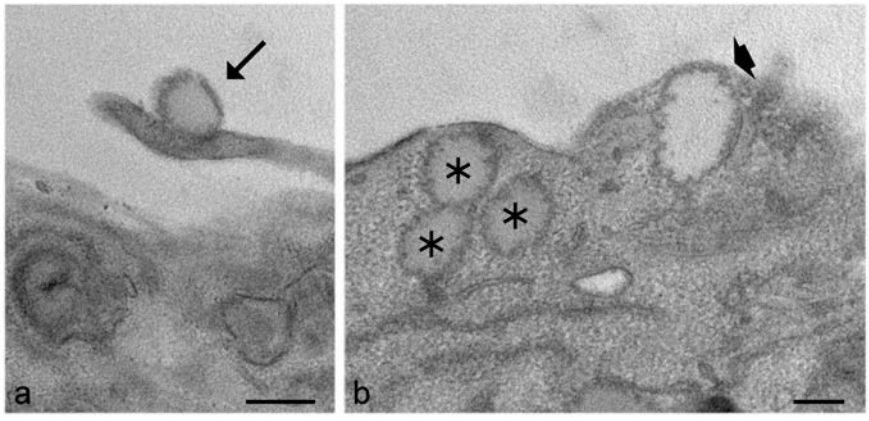

Figure 2. Transmission electron micrographs of C2C12 myoblasts, conventional ultrastructural morphology: a HA-NP (arrow) adheres to the cell surface (a) and residual bodies (asterisks) accumulate in the cytoplasm and sometimes bud from the cell surface (arrowhead) (b). Scale bars: 200 nm.

taraldehyde in PBS pH 7 for 30 min at room temperature, treated with AB as for light microscopy,[25] post-fixed with 1% OsO_4 for 1 h at room temperature, dehydrated with acetone and embedded in Epon resin as previously described.[29] As a control of staining specificity, some samples were processed as above described but, before AB treatment, the cells were incubated with 1 mg/ml of hyaluronidase (Sigma H3506) in normal saline for 1 h at room temperature. Ultrathin sections were observed without lead staining in a Philips Morgagni transmission electron microscope (FEI Company Italia Srl, Milan, Italy) operating at 80 kV and equipped with a Megaview II camera for digital image acquisition. The images were processed using Image-Pro Plus 7.0 software (Media Cybernetics Inc., Silver Spring, MD, USA).

Results and Discussion

HA-NPs showed a hydrodynamic size of 200 nm, a low PDI <0.1, and negative ζ potential ranging from -24 to -18 mV.

After AB staining in suspension, fluorescent HA-NPs (Figure 1a) appeared as blue dots at bright field microscopy (Figure 1b). Similarly, after NPs internalization in cultured cells, fluorescent HA-NPs appeared as bright green areas or spots (Figure 1c), while they appeared as blue clusters at bright field microscopy (Figure 1d). The overlapping of the blue staining with the green fluorescence signal demonstrated the specificity of the AB reaction for HA-NPs (Figure 1c,d). However, some AB-stained NPs did not match fluorescent NPs: this could be due to combined effect of the cell auto-fluorescence and the release of fluoresceinamine from NPs undergoing enzymatic degradation, which lowers NPs brightness, and the fluorescent signal occurring in the intracellular milieu, which masks NPs fluorescence. As for cell fluorescence, it should be underlined that C2C12 myoblasts show an intrinsic green auto-fluorescence that appeared to be increased after incubation with fluoresceinamine-labelled HA-NPs (*not shown*), thus supporting the hypothesis of the fluoresceinamine spreading following NPs degradation.

At TEM, the AB staining appeared as an irregular granular electron dense product, as Schofield *et al.* observed in cartilage samples.[25] In cells treated with HA-NPs, the AB staining was found on roundish structures with a moderate electron density corresponding to the NPs observed in unstained samples (Figure 2a) and to the size evaluated by dynamic light scattering. Stained NPs were observed adhering to the cell surface and inside invaginations of the plasma membrane (Figure 3 a,b). This evidence of the very early events in the NP uptake process was obtained thanks to the procedure of embedding cells as monolayers[29], which allows an optimal preservation of the spatial relationships between NPs and the plasma membrane. The AB staining was observed on intracellular NPs occurring either inside endosomes (Figure 3c) or free in the cytosol (Figure 3d). The occurrence of NPs free in the cytosol likely facilitates the release of fluorescent molecules, thus increasing the intracellular background visible at fluorescence microscopy.

The high concentration of HA in our NPs certainly promoted their intense AB-positivity at TEM. However, some AB staining was also clearly visible in large roundish structures (300 to 600 nm in diameter) occurring as clusters in the cytoplasm (Figure 3e), according to what observed in unstained samples (Figure 2b). We hypothesize that they represent NP residual bodies. In these residual bodies AB staining was preferentially located at the periphery, suggesting a compartmentalization of HA. To confirm the high sensitivity of AB staining at the ultrastructural level, the presence of HA was still recognizable as AB-positivity even when the residual bodies were found to be extruded from the cell (Figure 3f), probably due to NPs overloading.

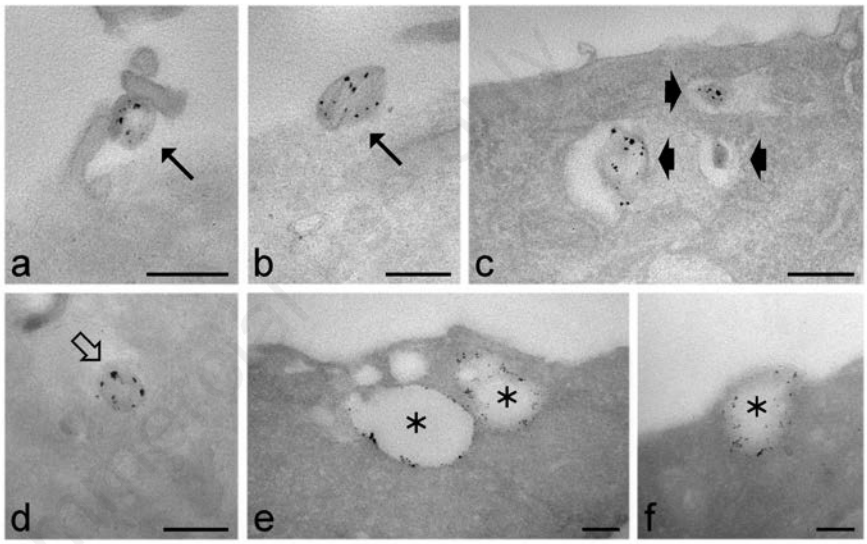

Figure 3. Transmission electron micrographs of C2C12 myoblasts after AB staining. a,b) The electron dense, granular reaction product occurs in HA-NPs (arrows) adhering to the cell surface. c) Three AB-stained HA-NPs are enclosed inside endosomes (arrowheads), just beneath the cell surface. d) A HA-NP free in the cytosol (open arrow) is clearly recognizable in the intracellular milieu. e) Residual bodies containing HA (asterisks) accumulate in the cytoplasm (e) and are extruded from the cell (f). Scale bars: 200 nm.

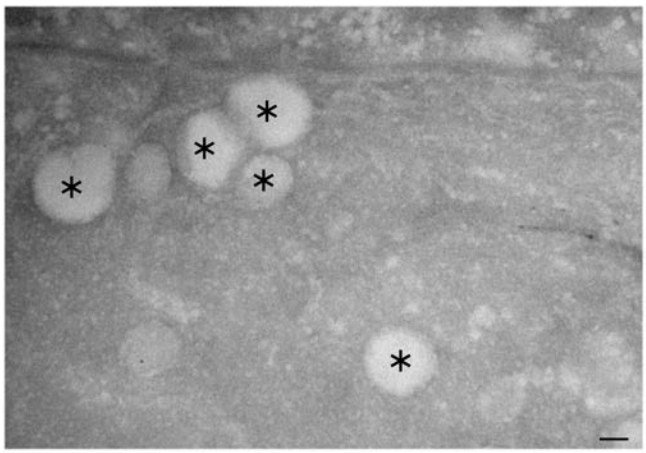

Figure 4. Sample treated with hyaluronidase as AB staining control: note the absence of any specific staining, especially in the residual bodies (asterisks). Scale bar: 200 nm.

No granular electron dense product was ever found in cells incubated with hyaluronidase before AB treatment, thus demonstrating the specificity of the staining procedure for HA at TEM (Figure 4). In addition, no granular reaction was observed in cell organelles of any cell samples or in control cells (not exposed to NPs), consistently with the evidence that intracellular HA is expressed only under particular condition such as inflammation.[30]

The overall appearance of AB-stained cells was similar as in samples routinely-processed for conventional ultrastructural morphology (Figure 2), although the intrinsic contrast was lower likely due to protein extraction during the staining at acid pH. Nevertheless, it is preferable to avoid the contrast-enhancing staining with lead citrate or uranyl acetate in samples treated with AB because both reagents produce a noisy fine pepper-like precipitate.

In addition to AB staining, other techniques have been developed for HA detection at the ultrastructural level, among which the periodic acid-Schiff method,[31-33] ruthenium red staining,[34] cationized ferritin binding,[35,36] high iron diamine method,[37] gold-conjugated hyaluronidase digestion,[38,39] labelled HA-binding probes.[40,41] These techniques often require special fixation procedures, whereas the AB staining is a simple and reliable method for the specific detection of HA in subcellular domains, which may be suitable for both light and electron microscopy under the usual fixation conditions for conventional ultrastructural morphology.

Our results demonstrated that the critical-electrolyte-concentration AB-staining is a powerful tool to thoroughly describe how HA-based NPs do interact with cells in culture, allowing to identify not only whole NPs while entering cells and moving into the cytoplasm, but also their remnants following lysosomal degradation and extrusion. This proves that this long-established staining method may successfully find application in a frontline research domain such as nanotechnology, namely for the ultrastructural study of scarcely electron-dense nanoconstructs that are especially promising drug carriers.

References

1. Lim CT, Han J, Guck J, Espinosa H. Micro and nanotechnology for biological and biomedical applications. Med Biol Eng Comput 2010;48:941-3. doi: 10.1007/s11517-010-0677-z
2. Lollo G, Rivera-Rodriguez GR, Bejaud J, Montier T, Passirani C, Benoit JP, et al. Polyglutamic acid-PEG nanocapsules as long circulating carriers for the delivery of docetaxel. Eur J Pharm Biopharm 2014;87:47-54. doi: 10.1016/j.ejpb.2014.02.004
3. Bobo D, Robinson KJ, Islam J, Thurecht KJ, Corrie SR. Nanoparticle-based medicines: a review of FDA-approved materials and clinical trials to date. Pharm Res 2016;33:2373-87. doi: 10.1007/s11095-016-1958-5
4. Fernandes RS, Dos Santos Ferreira D, de Aguiar Ferreira C, Giammarile F, Rubello D, de Barros AL. Development of imaging probes for bone cancer in animal models. A systematic review. Biomed Pharmacother 2016;83:1253-64. doi: 10.1016/j.biopha.2016.08.039
5. Kaur P, Aliru ML, Chadha AS, Asea A, Krishnan S. Hyperthermia using nanoparticles—Promises and pitfalls. Int J Hyperthermia 2016;32:76-88. doi: 10.3109/02656736.2015.1120889
6. Sasso MS, Lollo G, Pitorre M, Solito S, Pinton L, Valpione S, et al. Low dose gemcitabine-loaded lipid nanocapsules target monocytic myeloid-derived suppressor cells and potentiate cancer immunotherapy. Biomaterials 2016;96:47-62. doi: 10.1016/j.biomaterials.2016.04.010
7. Asadi N, Alizadeh E, Salehi R, Khalandi B, Davaran S, Akbarzadeh A. Nanocomposite hydrogels for cartilage tissue engineering: a review. Artif Cells Nanomed Biotechnol 2018;46:465-71. doi: 10.1080/21691401.2017.1345924
8. Kavoosi F, Modaresi F, Sanaei M, Rezaei Z. Medical and dental applications of nanomedicines. APMIS 2018;126:795-803. doi: 10.1111/apm.12890
9. Jahangirian H, Lemraski EG, Rafiee-Moghaddam R, Webster TJ. A review of using green chemistry methods for biomaterials in tissue engineering. Int J Nanomedicine 2018;13:5953-69. doi: 10.2147/IJN.S163399
10. Bamburowicz-Klimkowska M, Poplawska M, Grudzinski IP. Nanocomposites as biomolecules delivery agents in nanomedicine. J Nanobiotechnology 2019;17:48. doi: 10.1186/s12951-019-0479-x
11. Carton F, Chevalier Y, Nicoletti L, Tarnowska M, Stella B, Arpicco S, et al. Rationally designed hyaluronic acid-based nano-complexes for pentamidine delivery. Int J Pharm 2019;568:118526. doi: 10.1016/j.ijpharm.2019.118526
12. Suárez PL, García-Cortés M, Fernández-Argüelles MT, Encinar JR, Valledor M, Ferrero FJ, et al. Functionalized phosphorescent nanoparticles in (bio)chemical sensing and imaging - A review. Anal Chim Acta 2019;1046:16-31. doi: 10.1016/j.aca.2018.08.018
13. Wallyn J, Anton N, Akram S, Vandamme TF. Biomedical Imaging: Principles, Technologies, Clinical Aspects, Contrast Agents, Limitations and Future Trends in Nanomedicines. Pharm Res 2019;36:78. doi: 10.1007/s11095-019-2608-5
14. Boschi F, De Sanctis F. Overview of the optical properties of fluorescent nanoparticles for optical imaging. Eur J Histochem 2017;61:2830. doi: 10.4081/ejh.2017.2830
15. Poussard S, Decossas M, Le Bihan O, Mornet S, Naudin G, Lambert O. Internalization and fate of silica nanoparticles in C2C12 skeletal muscle cells: evidence of a beneficial effect on myoblast fusion. Int J Nanomedicine 2015;10:1479-92. doi: 10.2147/IJN.S74158
16. Marinozzi MR, Pandolfi L, Malatesta M, Colombo M, Collico V, Lievens PM, et al. Innovative approach to safely induce controlled lipolysis by superparamagnetic iron oxide nanoparticles-mediated hyperthermic treatment. Int J Biochem Cell Biol 2017;93:62-73. doi: 10.1016/j.biocel.2017.10.013
17. Pongrac IM, Ahmed LB, Mlinarić H, Jurašin DD, Pavičić I, Marjanović Čermak AM, et al. Surface coating affects uptake of silver nanoparticles in neural stem cells. J Trace Elem Med Biol 2018;50:684-92. doi: 10.1016/j.jtemb.2017.12.003
18. Steckiewicz KP, Barcinska E, Malankowska A, Zauszkiewicz-Pawlak A, Nowaczyk G, Zaleska-Medynska A, et al. Impact of gold nanoparticles shape on their cytotoxicity against human osteoblast and osteosarcoma in in vitro model. Evaluation of the safety of use and anti-cancer potential. J Mater Sci Mater Med 2019;30:22. doi: 10.1007/s10856-019-6221-2
19. Malatesta M, Giagnacovo M, Costanzo M, Conti B, Genta I, Dorati R, et al. Diaminobenzidine photoconversion is a suitable tool for tracking the intracellular location of fluorescently labelled nanoparticles at transmission electron microscopy. Eur J Histochem 2012;56:e20. doi: 10.4081/ejh.2012.20
20. Malatesta M, Pellicciari C, Cisterna B, Costanzo M, Galimberti V, Biggiogera M, Zancanaro C. Tracing nanoparticles and photosensitizing molecules at transmission electron microscopy by diaminobenzidine photo-oxidation. Micron 2014;59:44-51. doi: 10.1016/j.micron.2013.12.007
21. Morra M. Engineering of biomaterials surfaces by hyaluronan. Biomacromo-

lecules 2005;6:1205-23. doi: 10.1021/bm049346i
22. Micale N, Piperno A, Mahfoudh N, Schurigt U, Schultheis M, Mineo PG, et al. A hyaluronic acid–pentamidine bioconjugate as a macrophage mediated drug targeting delivery system for the treatment of leishmaniasis. RSC Adv 2015;5:95545-50. doi: 10.1039/C5RA18019H
23. Dosio F, Arpicco S, Stella B, Fattal E. Hyaluronic acid for anticancer drug and nucleic acid delivery. Adv Drug Deliv Rev 2016;97:204-36. doi: 10.1016/j.addr.2015.11.011
24. Scott JE, Dorling J. Differential staining of acid glycosaminoglycans (mucopolysaccharides) by alcian blue in salt solutions. Histochemie 1965;5:221-33. doi: 10.1007/ bf00306130
25. Schofield BH, Williams BR, Doty SB. Alcian Blue staining of cartilage for electron microscopy. Application of the critical electrolyte concentration principle. Histochem J 1975;7:139-49. doi: 10.1007/bf01004558
26. Fudala R, Mummert ME, Gryczynski Z, Rich R, Borejdo J, Gryczynski I. Lifetime-based sensing of the hyaluronidase using fluorescein labeled hyaluronic acid. J Photochem Photobiol B 2012;106:69-73. doi: 10.1016/j.jphotobiol.2011.10.005
27. Guglielmi V, Carton F, Vattemi G, Arpicco S, Stella B, Berlier G, et al. Uptake and intracellular distribution of different types of nanoparticles in primary human myoblasts and myotubes. Int J Pharm 2019;560:347-56. doi: 10.1016/j.ijpharm.2019.02.017
28. Costanzo M, Vurro F, Cisterna B, Boschi F, Marengo A, Montanari E, et al. Uptake and intracellular fate of biocompatible nanocarriers in cycling and noncycling cells. Nanomedicine (Lond) 2019;14:301-16. doi: 10.2217/nnm-2018-0148
29. Costanzo M, Malatesta M.. Embedding cell monolayers to investigate nanoparticle-plasmalemma interactions at transmission electron microscopy. Eur J Histochem 2019;63:3026. doi: 10.4081/ejh.2019.3026
30. Hascall VC, Majors AK, De La Motte CA, Evanko SP, Wang A, Drazba JA, et al. Intracellular hyaluronan: a new frontier for inflammation? Biochim Biophys Acta 2004;1673:3-12. doi: 10.1016/j.bbagen.2004.02.013
31. Scott JE, Harbinson RJ. Periodate oxidation of acid polysaccharides inhibition by the electrostatic field of the substrate. Histochemie 1968;14:215-20. doi: 10.1007/bf00306317
32. Scott JE, Harbinson RJ. Periodate oxidation of acid polysaccharides. II. Rates of oxidation of uronic acids in polyuronides and acid mucopolysaccharides. Histochemie 1969;19:155-61. doi: 10.1007/bf00281095
33. Scott JE, Dorling J. Periodate oxidation of acid polysaccharides. 3. A PAS method for chondroitin sulphates and other glycosamino-glycuronans. Histochemie 1969;19:295-301. doi: 10.1007/bf00279680
34. Luft JH. Ruthenium red and violet. I. Chemistry, purification, methods of use for electron microscopy and mechanism of action. Anat Rec 1971;171:347-68. doi: 10.1002/ar.1091710302
35. Eagles PA, Johnson LN, Van Horn C. The distribution of anionic sites on the surface of the chromaffin granule membrane. J Ultrastruct Res 1976;55:87-95. doi: 10.1016/s0022-5320(76)80084-6
36. Wessells NK, Nuttall RP, Wrenn JT, Johnson S. Differential labeling of the cell surface of single ciliary ganglion neurons in vitro. Proc Natl Acad Sci USA 1976;73:4100-4. doi: 10.1073/pnas.73.11.4100
37. Spicer SS, Hardin JH, Setser ME. Ultrastructural visualization of sulphated complex carbohydrates in blood and epithelial cells with the high iron diamine procedure. Histochem J 1978;10:435-52. doi: 10.1007/ bf0 1003007
38. Londoño I, Bendayan M. High-resolution cytochemistry of neuraminic and hexuronic acid-containing macromolecules applying the enzyme-gold approach. J Histochem Cytochem 1988;36:1005-14. doi: 10.1177/ 36.8. 3392391
39. Kan FW. High-resolution localization of hyaluronic acid in the golden hamster oocyte-cumulus complex by use of a hyaluronidase-gold complex. Anat Rec 1990;228:370-82. doi: 10.1002/ar.1092280403
40. Ripellino JA, Bailo M, Margolis RU, Margolis RK. Light and electron microscopic studies on the localization of hyaluronic acid in developing rat cerebellum. J Cell Biol 1988;106:845-55. doi: 10.1083/jcb.106.3.845
41. Eggli PS, Graber W. Association of hyaluronan with rat vascular endothelial and smooth muscle cells. J Histochem Cytochem 1995;43:689-97. doi: 10.1177/43.7.7608523